Nanosized iron clusters investigated with in situ transmission electron microscopy

Vystavel, T.; Palasantzas, G.; Koch, S. A.; de Hosson, J. Th. M.

Published in:
Applied Physics Letters

DOI:
10.1063/1.1536716

Publication date:
2003

Nanosized iron clusters investigated with *in situ* transmission electron microscopy

T. Vystavel, G. Palasantzas, S. A. Koch, and J. Th. M. De Hosson[a)]
Department of Applied Physics, Materials Science Centre and the Netherlands Institute for Metals Research, University of Groningen, Nijenborgh 4, 9747 AG Groningen, The Netherlands

(Received 2 October 2002; accepted 18 November 2002)

Transmission electron microscopy is employed for investigating the structural stability of nanosized iron clusters as deposited and after *in situ* annealing treatments under high vacuum conditions. The thin iron oxide shell that is formed around the iron clusters (upon air exposure) is of the order of 2 nm surrounding a 5 nm core of body-centered-cubic (bcc) iron. The oxide shell breaks down upon annealing at relatively low temperatures ($\sim 500\,^{\circ}\mathrm{C}$) leading to pure iron particles having a bcc crystal structure. Annealing of clusters, which are in contact, leads to their fusion and formation of larger clusters preserving their crystallographic structure and being free of any oxide shell. On the other hand, isolated clusters appear rather immobile (upon annealing). The truncated rhombic dodecahedron was found as the most probable shape of the clusters which differs from former theoretical predictions based on calculations of stable structural forms. © *2003 American Institute of Physics.* [DOI: 10.1063/1.1536716]

Recently, a strong impetus has been given to studies of nanocluster/nanostructured thin layers for two main reasons.[1–6] The first stems from the demand of miniaturization of electronic devices. Specifically, one would like to grow well-organized nanometer-size islands with specific electronic properties. The second reason finds its origin in tailoring nanostructured materials for specific mechanical and tribological properties that differ from their bulk counterparts. The precise reasons for these effects is currently under investigation, but one can cite the presence of a significant fraction of atoms in configurations different from the bulk, for example, in interfaces. In particular nanosized clusters are grown under nonequilibrium conditions, which allows one to obtain metastable systems. Because one avoids the effects of nucleation and growth on a specific substrate by direct cluster deposition, functional film properties may be tailored by choosing appropriate preparation conditions.

Especially, studies of nanometer scale magnetic clusters have been attractive because of the potential applications in high-density magnetic recording media. Because a large fraction of atoms in nanoclusters (sizes ~ 5 nm) are surface atoms, the thermal and magnetic properties[7–9] are quite different from the bulk counterparts. Although many investigations of low-temperature physical properties of magnetic nanoclusters have been performed,[10–16] only a few studies have been conducted on nanocluster properties at higher temperatures.[7,17] The latter are necessary because device operation might lead to heating and alteration of structural components that may affect the functional performance. Therefore, in this work, we study the structure of nanometer-size iron clusters and their response to high temperatures with *in situ* transmission electron microscopy (TEM) experiments.

Cluster deposition was performed using a NC200U nanocluster source manufactured by Oxford Applied Research.[2] It is based on the gas aggregation technique,[18] using a magnetron sputtering device to create an atomic vapor. The advantage of the method is that a relatively monodisperse size distribution can be produced. Sputtered atoms combine in a flow of rare gas (argon at a pressure 4×10^{-4} mbar) to form clusters. The chamber base pressure was $\sim 10^{-8}$ mbar, while during operation helium was also used as a cluster drift gas at a pressure $\sim 3\times10^{-5}$ mbar. The magnetron power was set to ~ 75 W (300 V and plasma current ~ 0.25 A). Clusters were deposited directly on Si_3N_4 and carbon support films of thickness 20 nm for TEM analysis.

The TEM analysis of the as-grown clusters indicates that an oxidation process occurs, as long as the sample is exposed to air even during sample transfer from the cluster source apparatus to the JEOL2010F transmission electron microscope. The typical cluster exhibited in Fig. 1 is composed of

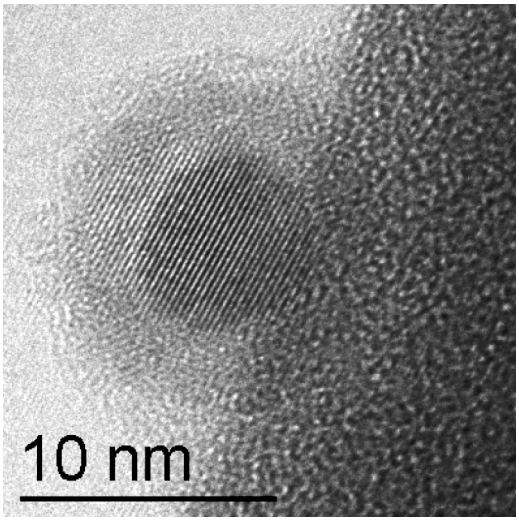

FIG. 1. TEM picture of one iron cluster exposed to air. Lattice fringes correspond well with {110} planes of bulk α-iron.

[a)]Author to whom all correspondence should be addressed; electronic mail: hossonj@phys.rug.nl

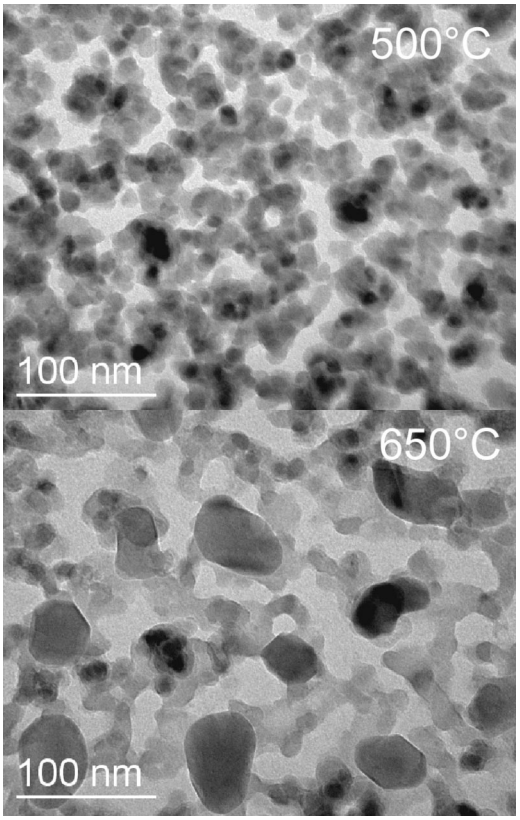

FIG. 2. Dense iron nanocluster film at 500 °C and 650 °C. At the latter temperature, nanocluster fusion takes place.

an iron oxide shell[19] with thickness approximately 2 nm and the iron core of typical diameter 5 nm. From electron diffraction studies as well as lattice spacing measurements of the metallic core, we conclude that the crystal structure corresponds to body-centered-cubic (bcc) iron.

However, the original shape of the clusters is altered by the oxide shell formation. For the type of oxide shell around the iron clusters, there are various possibilities. The most abundant form of iron oxide is γ-Fe_2O_3 (Ref. 20) while in the present system the Fe_3O_4 can not be excluded either. Indeed, Dupuis *et al.*[19] studied iron thin films (<100 nm) composed of 2–6 nm diameter clusters, and they found that 20% of their sample had been converted to both Fe_3O_4 and γ-Fe_2O_3. The oxidation of iron requires the addition of oxygen to the cluster, which results in an increase of the cluster size. However, the shell of oxide is thermally unstable due to its nanometer scale thickness (~ 2 nm) against even moderate cluster annealing at temperatures $T - T_{m\mathrm{Fe}}/3$, with $T_{m\mathrm{Fe}}$ as the melting temperature of bulk iron ($T_{m\mathrm{Fe}} = 1538$ °C).

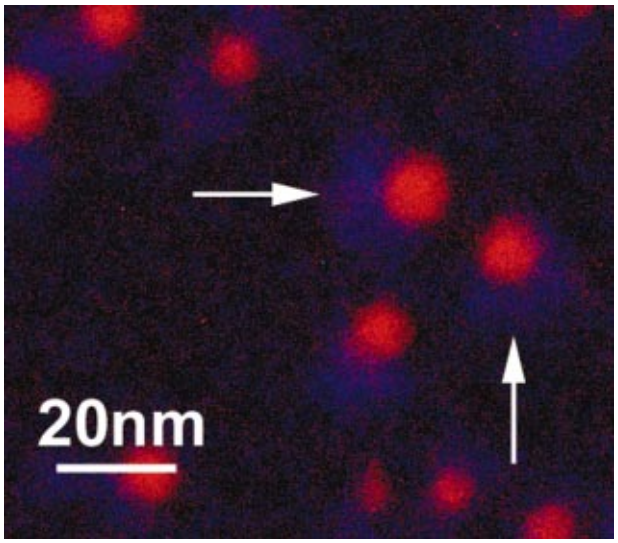

FIG. 3. (Color) TEM bright-field image and the corresponding elemental mapping by using energy filtered TEM (red: iron, blue: oxygen).

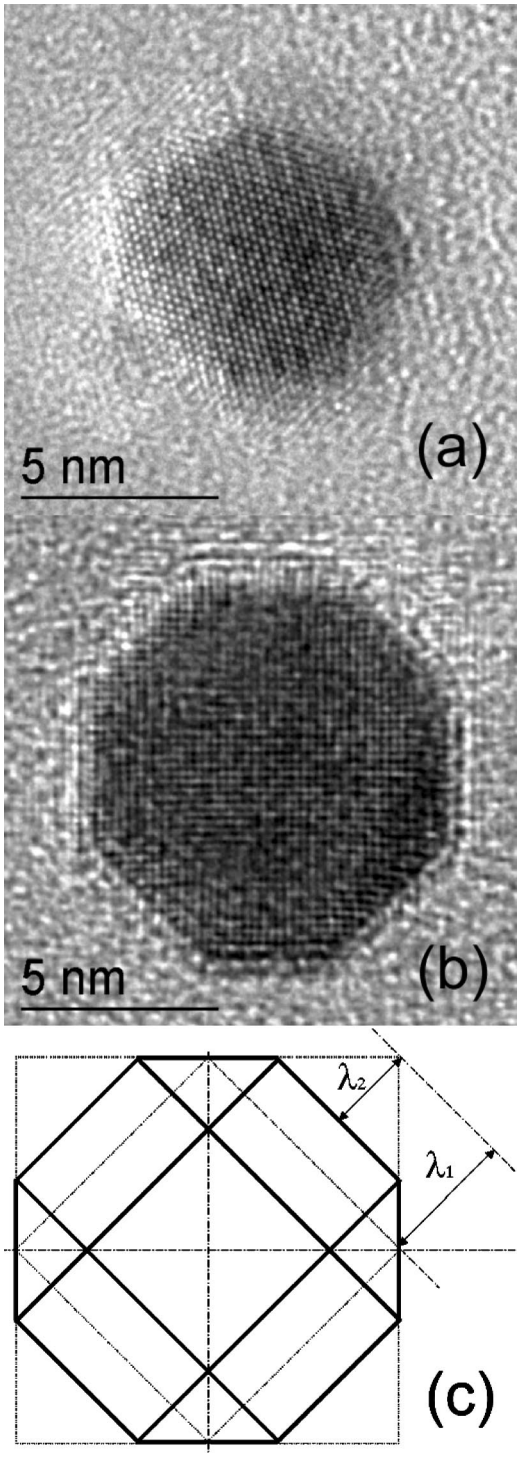

FIG. 4. Lattice imaging of two nanoclusters after *in situ* annealing in TEM. The iron oxide shell is decomposed. The clusters are oriented with respect to the electron beam as follows: (a) ⟨111⟩ bcc and (b) ⟨100⟩ bcc. (c) Drawings of ⟨100⟩ projection of truncated rhombic dodecahedron with schematic explanation of the truncation fraction λ_2/λ_1.

In situ TEM annealing at a pressure $\sim 10^{-4}$ mbar was

performed to study the development of the cluster structure. At 500 °C, cluster fusion starts to take place. Clusters that are in contact merge to form larger ones (see also Fig. 2), while isolated clusters stay intact and are rather immobile. There is no evidence for surface diffusion of the individual clusters. Figure 3 shows the decomposition of the iron oxide shell after annealing. In this case, no iron oxide phase is detectable either by elemental mapping or by diffraction studies. Nevertheless, an elemental map of oxygen indicates that oxygen-rich areas (without any iron present) remain on the surface beyond the iron cluster area, which is likely due to substrate oxidation (Fig. 3). In Fig. 3, a sample drift during elemental mapping can be excluded as the orientation of the oxygen-rich areas clearly indicates (arrows in Fig. 4). After annealing and thermal break up of the oxide shell that surrounds the iron clusters, the crystal structure of the remaining clusters still remains bcc.

The most stable structures[21] for medium-sized clusters (i.e., 100–10 000 atoms) calculated using an empirical many-body potential function are the bcc rhombic dodecahedron with 12 pseudoclose-packed {110} faces (having the lowest surface energy for bcc structures,[22] as is supported also by calculations using the density-functional theory),[23] and the icosahedron which is favorable for smaller clusters. A transition from icosahedron to bcc rhombic dodecahedron is predicted for cluster sizes of approximately 2000 atoms.[21] In addition, another possibility for stable iron clusters can be cuboctahedron [face-centered-cubic (fcc)] and truncated decahedron,[21] which could be feasible for clusters smaller than those in the present work.

Two typical cluster shapes observed after the *in situ* heating experiments are displayed in Fig. 4. The octahedral shape of the ⟨100⟩ projection [Fig. 4(b)] in combination with the ⟨111⟩ projection [Fig. 4(a)] leads to the conclusion that this shape corresponds to truncated rhombic dodecahedron, exposing 12 {110} faces, 6 {100} faces, and 8 {111} faces. The truncation of theoretically envisaged rhombic dodecahedron increases the spherical shape of the cluster although it also increases the fraction of the energetically less favorable faces. The degree of truncation can be described by the ratio λ_2/λ_1 [Fig. 4(c)] based on the Wulff construction. When $\lambda_2/\lambda_1=0$, there is no truncation of the rhombic dodecahedron, while when $\lambda_2/\lambda_1=1$, we have a fully truncated shape, i.e., a cuboctahedron. An average experimental value of the λ_2/λ_1 fraction is $\lambda_2/\lambda_1=0.565\pm0.05$, which yields the fraction of surface energies $\gamma_{100}/\gamma_{110}=1.02$ if we use the relation $\lambda_2/\lambda_1=2-\sqrt{2}(\gamma_{100}/\gamma_{110})$ for rhombic dodecahedron. This result confirms comparable surface energies of {100} and {110} planes found by quantum-mechanical calculations.[23]

In conclusion, we investigated the structural evolution due to annealing treatments of iron nanoclusters by means of TEM. The thin layer of iron oxide formed around the iron clusters is of the order of 2 nm surrounding a 5 nm core of bcc iron. Such an oxide shell breaks down at relatively low temperatures ~500 °C leading to pure iron particles. Annealing of clusters in contact leads to fusion and formation of larger clusters (preserving their crystallographic structure) free of oxide. On the other hand, isolated clusters appear rather immobile. Finally, structural characteristics of reformed clusters (either isolated or generated by fusion of other clusters) differ from former theoretical predictions regarding calculations of stable structural forms[21] since our results favor truncated polyhedron for relatively large cluster sizes. The theoretical calculations concern static properties at 0 K of free clusters, ignoring temperature effects and cluster dynamics.[21] The latter is not expected to play a major role in our case since the ratio $\gamma_{100}/\gamma_{110}$ is close to that of the Wulff construction, while any influence arising from the presence of a substrate is also excluded.

The authors would like to acknowledge financial support from the Materials Science Center (MSC^+) program and the Netherlands Institute for Metals Research.

[1] C. Binns, Surf. Sci. Rep. **44**, 1 (2001).
[2] H. Haberland, M. Moseler, Y. Qiang, O. Rattunde, T. Reiners, and Y. Thurner, Surf. Rev. Lett. **3**, 887 (1996).
[3] G. Fuchs, P. Melinon, F. S. Aires, M. Treilleux, B. Cabaud, and A. Hoareau, Phys. Rev. B **44**, 3926 (1991).
[4] P. Jensen, Rev. Mod. Phys. **71**, 1695 (1999).
[5] R. L. Johnston, Philos. Trans.: Math. Phys. Eng. Sci. **356**, 211 (1998).
[6] C. G. Zimmermann, M. Yeadon, K. Nordlund, J. M. Gibson, and R. S. Averback, Phys. Rev. Lett. **83**, 1163 (1999).
[7] Y. D. Yao, Y. Y. Chen, C. M. Hsu, H. M. Lin, C. Y. Tung, M. F. Tai, D. H. Wang, K. T. Wu, and C. T. Suo, Nanostruct. Mater. **6**, 933 (1995).
[8] Y. Y. Chen, Y. D. Yao, C. R. Wang, W. H. Li, C. L. Chang, T. K. Lee, T. M. Hong, J. C. Ho, and S. F. Pan, Phys. Rev. Lett. **84**, 4990 (2000).
[9] J. F. Löffler, H.-B. Braun, and W. Wagner, Phys. Rev. Lett. **85**, 1990 (2000).
[10] C. Binns, S. H. Baker, M. J. Maher, S. Louch, S. C. Thornton, K. W. Edmonds, S. S. Dhesi, and N. B. Brookes, Phys. Status Solidi A **189**, 339 (2002).
[11] S. Gangopadhyay, G. C. Hadjipanayis, S. I. Shah, C. M. Sorensen, K. J. Klabunde, V. Papaefthymiou, and A. Kostikas, J. Appl. Phys. **70**, 5888 (1991).
[12] W. Gong, H. Li, Z. Zhao, and J. Chen, J. Appl. Phys. **69**, 5119 (1991).
[13] S. Gangopadhyay, G. C. Hadjipanayis, B. Dale, C. M. Sorensen, K. J. Klabunde, and A. Kostikas, Phys. Rev. B **45**, 9778 (1992).
[14] S. Gangopadhyay, G. C. Hadjipanayis, C. M. Sorensen, and K. J. Klabunde, J. Appl. Phys. **73**, 6964 (1993).
[15] F. Bødker, S. Mørup, and S. Linderoth, Phys. Rev. Lett. **72**, 282 (1994).
[16] M. Holdenried, B. Hackenbroich, and H. Micklitz, J. Magn. Magn. Mater. **231**, L13 (2001).
[17] Y. D. Yao, Y. Y. Chen, S. F. Lee, W. C. Chang, and H. L. Hu, J. Magn. Magn. Mater. **239**, 249 (2002).
[18] C. G. Granqvist and R. A. Buhrman, J. Appl. Phys. **47**, 2200 (1976).
[19] V. Dupuis, J. P. Perez, J. Tuaillon, V. Paillard, P. Mélinon, A. Perez, B. Barbara, L. Thomas, S. Fayeulle, and J. M. Gay, J. Appl. Phys. **76**, 6676 (1994).
[20] M. D. Upward, B. N. Cotier, P. Moriarty, P. H. Beton, S. H. Baker, C. Binns, and K. Edmonds, J. Vac. Sci. Technol. B **18**, 2646 (2000).
[21] N. A. Besley, R. L. Johnston, A. J. Stace, and J. Uppenbrink, J. Mol. Struct.: THEOCHEM **341**, 75 (1995).
[22] D. Wolf, Philos. Mag. A **63**, 337 (1991).
[23] M. J. S. Spencer, A. Hung, I. K. Snook, and I. Yarovsky, Surf. Sci. **513**, 389 (2002).